

Stimulated Photon-Echo and Transient-Grating Studies of Protein-Matrix Solvation Dynamics and Interexciton-State Radiationless Decay in α Phycocyanin and Allophycocyanin

Bradley J. Homoelle, Maurice D. Edington,[†] William M. Diffey, and Warren F. Beck*

Department of Chemistry, Vanderbilt University, 5134 Stevenson Center, Post Office Box 1822-B, Nashville, Tennessee 37235

Received: August 26, 1997; In Final Form: February 10, 1998

We have employed two third-order femtosecond spectroscopic methods, stimulated-photon-echo peak-shift (3PEPS) and transient-grating (TG) spectroscopy, to characterize solvation dynamics and interexciton-state radiationless decay in the α subunit of *C*-phycocyanin and in allophycocyanin. The α subunit contains a single phycocyanobilin chromophore in an isolated protein-matrix environment. Allophycocyanin contains exciton-coupled pairs of phycocyanobilins in the same type of binding site found in the α subunit. The results show that both systems exhibit a biphasic solvation response: the inertial phase, arising from librational motions of the amino acids or included water molecules in the phycocyanobilin-binding site, contributes a 80–100-fs component to the 3PEPS profile and appears as a rapidly damped 72-cm⁻¹ modulation of the TG signal; the diffusive phase, arising from collective protein-matrix motions, contributes a component in the TG signal and 3PEPS profile on the 5–20-ps time scale. Both systems exhibit nearly instantaneous (16-fs) components in the 3PEPS profiles that arise from intrachromophore vibrational modes. The 3PEPS profile observed with allophycocyanin exhibits additional fast decay components, with time constants of 56 and 220 fs, that apparently report the contributions to electronic dephasing arising from radiationless decay between imperfectly correlated exciton states. The TG signal evidences vibrational relaxation in the lower exciton state and incoherent energy transfer between the chromophores in a given pair. The results present complementary details on solvation and interexciton-state radiationless decay dynamics that were first observed in this laboratory using time-resolved pump–probe and anisotropy methods.

Introduction

In recent work, Fleming and co-workers^{1–5} have applied two third-order spectroscopic methods, the three-pulse stimulated-photon-echo peak-shift (3PEPS) measurement⁶ and transient-grating (TG) spectroscopy,⁷ to the characterization of solvation dynamics around fluorescent chromophores in molecular liquids, polymer hosts, and proteins. Wiersma and co-workers^{8–10} have pioneered time-resolved (or gated) versions of the 3PEPS experiment. The 3PEPS technique, in particular, may permit a distinction of the inertial solvation response^{11–16} from the typically faster part of the Stokes shift that involves displacement of intrachromophore vibrational modes.^{3–5} The inertial response is thought to involve librational motions of the first solvent shell that surrounds a chromophore.¹⁶ We have suggested that the inertial response in proteins probably involves motions of the side chains of the amino acids or any included water molecules that form the lining of the binding site of a chromophore or reactive center.^{17–19}

This paper presents an application of the 3PEPS and TG techniques to the internal solvation response and excited-state dynamics of two photosynthetic light-harvesting systems obtained from the phycobilisome of cyanobacteria,²⁰ the α subunit of *C*-phycocyanin and allophycocyanin in the trimeric aggregation state. The crystal structures of *C*-phycocyanin and allo-

phycocyanin have been determined by using X-ray diffraction methods by Huber and co-workers.^{21–24} As shown in Figure 1, the isolated α subunit contains a single phycocyanobilin (open-chain tetrapyrrole) chromophore; the trimeric aggregation state of allophycocyanin organizes phycocyanobilin chromophores into exciton-coupled pairs.

We previously employed femtosecond time-resolved hole-burning spectroscopy to characterize both of these systems.^{18,26–29} By comparing the response observed in the two systems, we were able to distinguish the dynamics associated with chromophore–chromophore interactions in allophycocyanin from those associated with chromophore–protein interactions. The work on the α subunit suggests the presence of an inertial solvation response, but the analysis of the transiently hole-burned line shapes did not permit a distinction to be made between the part of the dynamic Stokes shift that involves vibrational displacement and that of solvation.¹⁸ The results obtained with allophycocyanin showed that delocalized excited states are initially present;^{26,27} extremely fast (30–50-fs time constant) radiationless-decay processes transfer population between the two exciton states at room temperature.^{26–28}

The 3PEPS and TG results described in this paper provide firm evidence for the first time that proteins exhibit an inertial solvation response. Both of the target systems exhibit nearly identical phases of 3PEPS response that are assigned to intrachromophore vibrational modes and inertial solvation. The α subunit exhibits a long-lived component in the 3PEPS profile and TG signal that arises from a diffusional solvation response

[†] Present address: Department of Chemistry, Duke University, Post Office Box 90349, Durham, NC 27708.

* Corresponding author: phone and fax, 615-343-0348; e-mail, warren.f.beck@vanderbilt.edu.

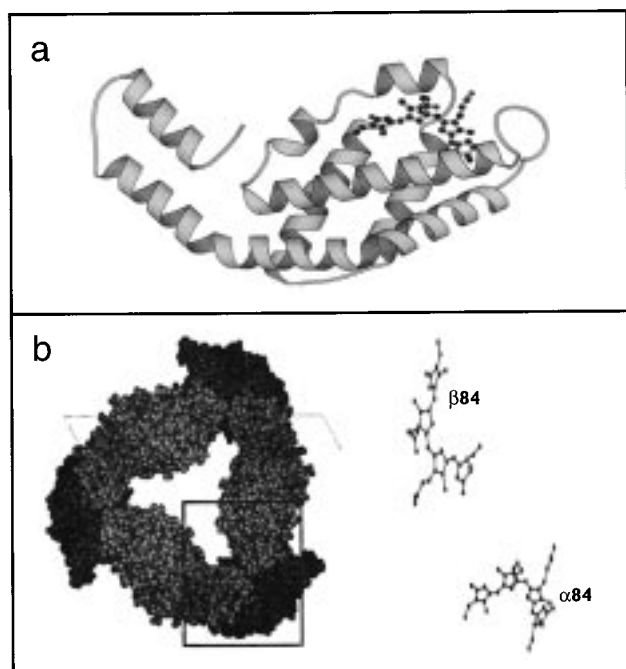


Figure 1. Structures of (a) the α subunit of C-phycoerythrin and (b) allophycocyanin trimers, as described in the X-ray crystal structures determined by the Huber group.^{21–24} The ribbon diagram in (a) was generated with the MOLSCRIPT program.²⁵

on the picosecond time scale and an even longer lived inhomogeneity. At least the picosecond part of the solvent response is analogous to the dielectric relaxation observed in molecular liquids that arises from rotational diffusion,^{30–32} but in proteins the diffusional response has to involve longer-range conformational motions. In addition to the intrinsic dynamics of a single-chromophore system, allophycocyanin exhibits additional fast contributions to the decay of the 3PEPS profile that have to do with radiationless transfer of population between its exciton states. The TG response exhibits components from vibrational relaxation in the lower exciton state and incoherent energy transfer between the chromophores in a given exciton-coupled pair. The results obtained in this work from the two third-order spectroscopies are complementary but superior in several ways to the results obtained previously in this laboratory using femtosecond transient hole-burning spectroscopy.

Experimental Section

Sample Preparation. α subunits of C-phycoerythrin were isolated from the AN112 mutant of the cyanobacterium *Synechococcus* PCC 6301 by using previously described methods.³³ C-Phycocyanin hexamers were purified by ion-exchange chromatography on a DEAE-cellulose column.³³ α subunits were obtained by denaturing the protein in urea-containing buffer solutions and then separating the α - and β -subunits on a Bio-Rex-70 ion-exchange column (BioRad), as previously described by Glazer and co-workers.³⁴ The isolated α subunits were stored as dilute solutions (<0.01 absorbance, as measured at 620 nm in a 1-cm cuvette) in the dark; the storage solution was a 5 mM phosphate buffer solution at pH 7. On the day of an experiment, the dilute α subunits were concentrated at 4 °C in an stirred Amicon ultrafiltration cell over a PM-10 membrane or in an Amicon Centrprep-3 concentrator centrifuged at 4500 rpm in a Sorvall GSA rotor in a RC-5B centrifuge.

Analysis of the purified C-phycoerythrin subunits by SDS-polyacrylamide gel electrophoresis showed that the α - and

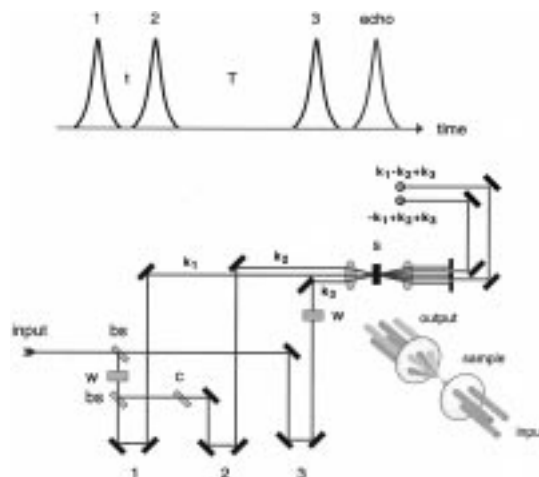


Figure 2. (Top) Pulse sequence and interpulse time variables used in the 3PEPS and TG experiments. (Bottom) Schematic diagram of the three-pulse modified Mach-Zender interferometer used in the 3PEPS and TG experiments. Symbols: bs, beam splitter; w, $\lambda/2$ plate and Glan-laser calcite polarizer, in sequence; c, compensator plate; s, sample cell. Beam 1 is chopped by a mechanical chopper. The two echo or grating beams pass through Glan-laser calcite polarizers before hitting the photodiode detectors. The inset shows the forward box geometry used for the incident beams and the positions of the two phase-matched echo or grating beams that are simultaneously detected.

β -subunit fractions were free of contamination from the other polypeptide. Although Glazer and co-workers³⁵ reported that α -subunit preparations self-associate into α_2 dimers upon renaturation in urea-free buffer solutions, our α -subunit preparations run as monomers on a HPLC size-exclusion column (Rainin Hydropore-5-SEC) at room temperature at injection concentrations comparable to those used for femtosecond spectroscopy; elution of protein was monitored at 280 nm, while the phycocyanobilin chromophore was monitored at 620 nm. The aggregation state and solvatochromism of the α -subunit preparations prepared according to our methods have been discussed in detail in another article.¹⁹

Allophycocyanin trimers were also isolated from cultures of the AN112 mutant of *Synechococcus* PCC 6301, as described elsewhere.^{27,33} The samples were stored in the dark at 4 °C suspended in a 100 mM sodium phosphate buffer solution at pH 7.0.

Femtosecond Spectroscopy. The photon-echo and transient-grating results described in this paper were obtained with an amplified colliding-pulse, mode-locked (CPM) dye laser, described in detail in previous work,¹⁸ and a three-pulse modified Mach-Zender interferometer based in part on the design reported previously by Fleming and co-workers.¹ The output of the amplified CPM laser was used directly after compensation for group-delay dispersion with a pair of fused-silica prisms. Neutral-density filters were used to attenuate the energy of each of the three beams to the 10 nJ/pulse level (at 3 kHz), as measured at the sample's position. The cross-correlation waveform obtained with two of the beams exhibited 140-fs widths (fwhm), which implies that the pulses exhibit 90-fs widths if a sech^2 profile is assumed. The spectrum was 6 nm wide and centered at 622 nm.

Our implementation of the Fleming group's¹ design for the three-pulse photon-echo/transient-grating spectrometer is depicted in Figure 2. The pulse train from the amplified CPM laser is divided by a sequence of two beam splitters into three beams. Each beam encounters the same number and type of transmissive optics on the way to the sample position, so the

single pair of prisms prior to the interferometer can be used to compensate for the group-delay dispersion in all three beams. The time-of-flight delay to the sample position is controlled by two computer-controlled translation stages: the delay for pulse 2 uses a Newport 850B actuator and Newport/Klinger steel stage under the control of a Newport PMC 200-P controller, and the delay for pulse 3 is controlled by a Melles-Griot steel stage equipped with a Nanomover actuator and controller. The polarization direction and relative intensity of the three beams is controlled by an achromatic $\lambda/2$ waveplate (Optics for Research) and a calcite Glan-laser polarizer (Karl Lambrecht), in sequence. Two of the beams (for pulses 1 and 2) share the same polarization orientation, while the plane of polarization of pulse 3 is made perpendicular to that of pulses 1 and 2. A 10-cm fused-silica singlet objective focuses the beam onto the sample position, and a 20-cm BK7 singlet objective is used to recollimate the exiting beams.

The forward box geometry, consisting of an equilateral triangle for the spacing of the three incident beams, was used as described by Fleming and co-workers¹ to obtain spatial resolution of the photon-echo or transient-grating signals from the transmitted input beams. The 3PEPS and TG experiments are conducted with the same configuration; both methods involve detection of coherently radiated beams along the $\vec{k}_1 - \vec{k}_2 + \vec{k}_3$ and $-\vec{k}_1 + \vec{k}_2 + \vec{k}_3$ directions, where \vec{k}_i represents the direction of incidence. A pair of amplified photodiodes (Thorlabs) and digital lock-in amplifiers (SRS) are employed to detect the two beams simultaneously. Prior to hitting the photodiode detectors, each signal beam passes through spatial filters (prior to recollimation and along a 1-m flight path) and a Glan-laser calcite polarizer, which is oriented to pass the direction parallel to beam 3's plane of polarization.¹

The sample was recirculated through a 0.1-mm fused-silica flow cuvette at the maximum flow rate (0.5 mL/min) that could be achieved without causing turbulence. The concentration of the sample was adjusted to establish an absorption of 0.2–0.4 for the 0.1-mm path, as measured at 620 nm. The samples were extensively centrifuged (at least 30 min at 40000g in a Sorvall SS-34 rotor and RC-5B centrifuge) and then passed through a 0.22- μ m microfilter prior to use.

Results

Figure 3 compares the continuous ground-state absorption spectra obtained from the α subunits and from allophycocyanin trimers at room temperature. The bottom panel shows the putative exciton-state absorption line shapes determined by Maurice Edington in this laboratory based on an analysis of femtosecond time-resolved pump–probe absorption-difference spectra.^{26–28} The spectrum of the 90-fs (sech^2) laser pulses used in the photon-echo and transient-grating studies is centered at 622 nm; it pumps the α subunits within 150–200 cm^{-1} of the 0–0 transition. The pump spectrum prepares a $\sim 3:1$ ratio of the two exciton states in allophycocyanin.

Figure 4 shows examples of three stimulated-photon-echo signals obtained with α -subunit preparations at room temperature, as scanned with respect to the delay t between the first and second pulses at fixed delays T between the second and third pulses. The observed echo traces were fit to Gaussian profiles by using nonlinear least-squares techniques. The traces are described well by Gaussian line shapes except near $T = 0$ fs, where there is a discernible asymmetry. The peak shift (3PEPS) is determined as one-half the difference between the peak maxima. The three signals shown in Figure 4 indicate that the peak shift decays rapidly during the first 100 fs but that a long-lived shift remains at $T = 1000$ fs.

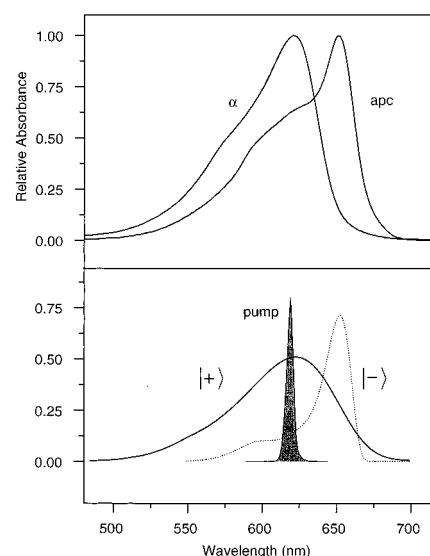


Figure 3. (Top panel) Continuous ground-state absorption spectra obtained from the α subunits and from allophycocyanin trimers at room temperature. The spectral band-pass was 2 nm. (Bottom panel) Exciton-state absorption component line shapes for the absorption spectrum of allophycocyanin trimers, for the upper exciton state ($|+\rangle$, solid curve) and for the lower exciton state ($|-\rangle$, dotted curve) as obtained from an analysis of femtosecond time-resolved pump–probe absorption-difference spectra at room temperature, as previously reported.^{26–28} Also shown is the spectrum of the 90-fs (sech^2) pulses (shaded narrow curve) that were used in the 3PEPS and TG experiments, as obtained directly from the amplified CPM laser.

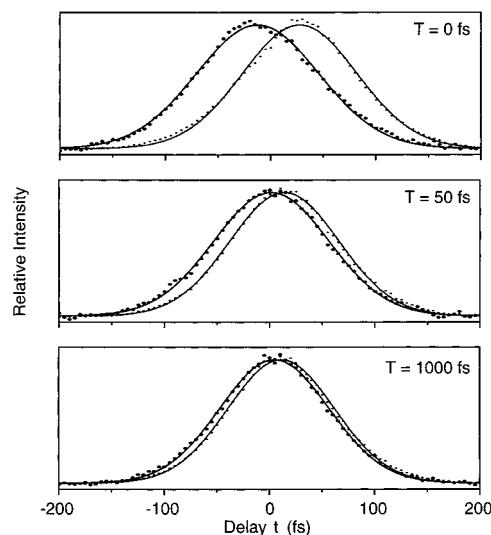


Figure 4. Examples of three 3PEPS scans (in the t dimension) obtained with α -subunit preparations at room temperature at $T = 0$, 50, and 1000 fs. The two traces represent the echo signals obtained from the two phase-matched directions. The traces are superimposed with fits to Gaussian line shapes, as determined by a nonlinear least-squares regression routine.

Figure 5 shows the complete 3PEPS profiles as a function of delay T for α -subunit preparations (filled circles) and for allophycocyanin trimers (open circles), both obtained at room temperature. The peak shift is plotted on a logarithmic vertical axis. This plot permits one to discern directly several regimes of exponential decay in each 3PEPS profile. Both preparations exhibit the same peak shift at $T = 0$ fs within 0.3 fs. The initial decay, on the 0–20-fs time scale, is almost identical in the two preparations, but the two profiles diverge at $T = 25$ fs. The profile obtained with allophycocyanin trimers exhibits a much faster decay over the 25–200-fs delay range than does the one

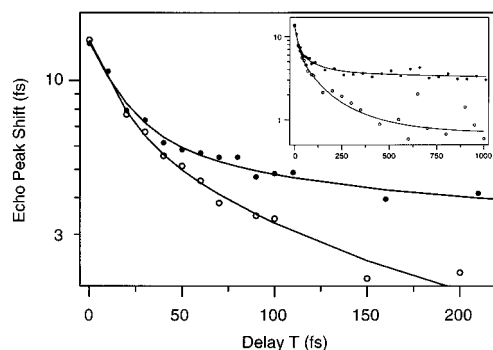


Figure 5. 3PEPS profiles as a function of delay T for α -subunit preparations (filled circles) and for allophycocyanin trimers (open circles), both obtained at room temperature. Note that the peak shift is plotted on a logarithmic axis. The inset shows the same profiles over the 0–1000-fs delay range. The curves drawn through the data points were obtained from nonlinear least-squares fits to multiexponential models. The fit parameters are shown in Tables 1 and 2.

TABLE 1: Exponential Fit Components for the 3PEPS Profile Observed at Room Temperature with α -Subunit Preparations

	amplitude, fs	time constant, fs	assignment
1	6.7 ± 0.91	17 ± 7.8	intrachromophore vibrational modes
2	3.0 ± 0.44	97 ± 27	inertial protein-matrix solvation
3	2.8 ± 0.19	5500 ± 4600	diffusive protein-matrix solvation
4	0.91 ± 0.18	nondecaying	long-lived inhomogeneity

TABLE 2: Exponential Fit Components for the 3PEPS Profile Observed at Room Temperature with Allophycocyanin Trimers

	amplitude, fs	time constant, fs	assignment
1	6.3 ± 0.95	16 ± 4.8	intrachromophore vibrational modes
2	1.7 ± 0.63	56 ± 34	interexciton-state radiationless decay
3	2.6 ± 0.33	81 ± 32	inertial protein-matrix solvation
4	2.4 ± 0.22	220 ± 81	interexciton-state radiationless decay
5	0.70 ± 0.19	nondecaying	diffusive protein-matrix solvation, on > 10-ps time scale, and/or long-lived inhomogeneity

obtained with α -subunit preparations. Note, however, that the slope of the decay observed over the 20–50-fs delay region in the α -subunit profile is very similar to that of the allophycocyanin profile over the 40–150-fs delay region. A slow decline is detected in the α -subunit profile that extends at least out to the 1000-fs delay. The raw profiles exhibit a substantial gap at the 1000-fs delay, with the observed peak shift remaining well above 3 fs for the α -subunit profile. The noise level on the 3PEPS profile obtained with allophycocyanin trimers is substantially higher than that for the α -subunit profile over the 200–1000-fs delay range owing to the rapid decrease in absolute echo intensity caused by the population decay that arises from interexciton-state radiationless decay and vibrational relaxation.

To obtain a rough division of the 3PEPS profiles into components to facilitate discussion, the profiles were fit to a multiexponential model by using a nonlinear least-squares regression program. Tables 1 and 2 show the fit parameters for the smooth curves drawn through the 3PEPS data points in Figure 5. The profile obtained for the α subunit is adequately described by three exponentials and a long-lived offset; a four-exponential model produced a fit with two of the components having the same time constant. The profile for allophycocyanin trimers requires four distinct exponential components and an offset. The two fits were obtained without constraints on the fit parameters. As indicated by the direct examination of the

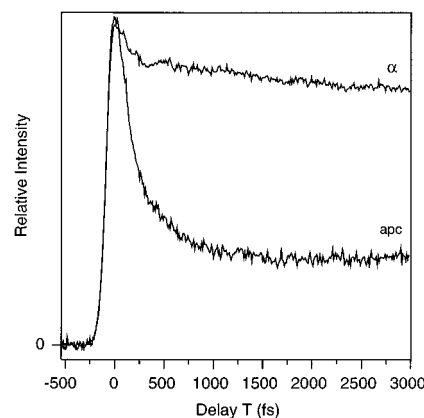


Figure 6. Transient grating signals obtained at room temperature with α -subunit preparations (α) and with allophycocyanin trimers (apc). The two traces were normalized to approximately the same maximum intensity near zero time.

3PEPS profiles given above, the two profiles exhibit two components that are identical, within experimental error. The fastest component exhibits a ~ 6.5 -fs amplitude and a ~ 16 -fs time constant in both systems. A component with a time constant of 80–100 fs and a ~ 2.7 -fs amplitude is also present for both systems. In addition to these components, allophycocyanin exhibits components with ~ 56 - and ~ 220 -fs time constants, while the α subunits exhibit a slower component with a ~ 5.5 -ps time constant that is poorly defined by the fitted 0–1000-fs data set. Experiments with the delay T scanned over the 0–100-ps time scale suggest that the ~ 3 -fs shift at $T = 1000$ fs exhibited by the α subunit does not significantly decay.

Figure 6 compares the TG signals obtained at room temperature with α -subunit preparations and with allophycocyanin trimers. These signals were obtained with the delay t set to zero, as determined by cross-correlation experiments, and with the delay T scanned. The two traces exhibit an identical rise, as limited by the duration of the 90-fs laser pulses used in the experiment. Notice, however, that the trace obtained with the α -subunit preparations exhibits only a $\sim 10\%$ decay over the first 200 fs and that weak oscillations are observed over at least the ~ 0 –500-fs time scale. The TG trace observed with allophycocyanin trimers exhibits a large decay over the 0–1000-fs delay region that is not observed with the α -subunit preparations. This decay is associated with radiationless decay between exciton states, with vibrational relaxation in the lower exciton state, and with incoherent energy transfer between the nonidentical chromophores in a given pair.²⁷

The decaying, modulated portion of the TG transient obtained with the α subunits was fit to a series of damped cosinusoids of the form $a_0 \exp(-t/\tau) \cos(\omega t + \phi)$ by a linear-prediction, singular-value-decomposition (LPSVD) procedure.^{36,37} The transient was analyzed starting at a delay of 75 fs past time zero. The program we used to perform the LPSVD analyses was a modified version of one that was generously provided to us by Professor Anne Myers (University of Rochester); an application of this LPSVD program to an analysis of resonant impulsive stimulated Raman (RISRS) transients was published by Johnson and Myers.³⁷ Figure 7 shows that the first 750 fs of the TG signal exhibits modulations; the LPSVD fit consists of a sum of two rapidly damped cosinusoids, with frequencies of 72 and 249 cm^{-1} , and an exponential decay. Table 3 shows the fit parameters. The 72- cm^{-1} component is apparently responsible for the main structure observed in the TG transient, but the 249- cm^{-1} component is required to account for structure above the noise level on the initial fast decline of the signal.

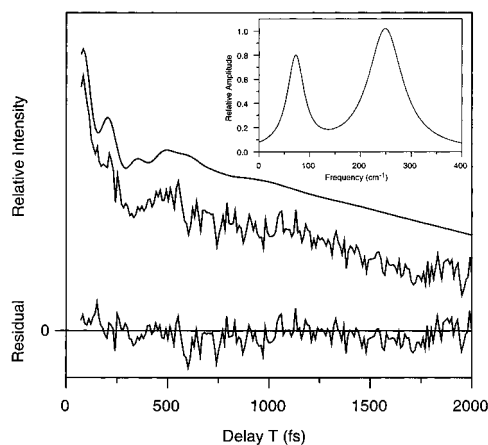


Figure 7. Linear prediction, singular-value decomposition (LPSVD) fit of the decay and modulations observed in the TG signal from α -subunit preparations. The smooth trace offset vertically from the experimental TG signal is the LPSVD fit. The residual (data - fit) is shown in the bottom part of the main panel. The inset shows a spectral representation of the oscillatory part of the LPSVD fit, which consists of a sum of two damped cosinusoids and an exponential decay; the fit parameters are listed in Table 3.

TABLE 3: LPSVD Fit Components for the TG Signal Obtained at Room Temperature with α -Subunit Preparations

frequency, cm^{-1}	damping constant, fs	phase, deg	rel amplitude
0	20000	0	13.8
72	264	90	0.75
249	130	-51	1.0

Given that 90-fs pulses were used in the TG experiment, it is likely that the extremely short dephasing time of this latter component is a manifestation of the unresolved higher frequency components that are coupled to the electronic transition but are not impulsively excited. The strongest mode in the UV-excited resonance Raman spectrum, for instance, is a $\sim 1500\text{-cm}^{-1}$ mode corresponding to a pyrrole-stretching vibration;³⁸⁻⁴⁰ this mode apparently provides the main progression that imparts a weak vibronic structure to the ground-state absorption spectrum.

Because modulations are not as obvious in the TG signal observed with allophycocyanin trimers, we used a nonlinear least-squares routine to obtain just a description of the decay. Figure 8 shows the decaying portion of the TG signal along with a fit to two exponentials and a long-lived offset; notice that the top part of Figure 8 is drawn according to a logarithmic vertical axis. The decay is best described as being nonexponential rather than multiexponential because there are no sustained delay regions that exhibit a linear decline, as presented with the logarithmic vertical axis. The parameters for a double-exponential fit are listed in Table 4; the fast component exhibits a 160-fs time constant, while the slower exponential exhibits a 430-fs time constant.

Owing to the modulus-squared nature of the TG signal, these time constants should be multiplied by a factor of 2 when compared to those of exponential kinetic time constants in pump-probe experiments or to those in the 3PEPS profiles.^{1,3} The residual shown in the bottom part of Figure 8 shows that the double-exponential model fails to describe a weak modulatory character over the first 750 fs of delay that is similar to the 72-cm^{-1} modulation observed in the TG transient obtained with the α -subunit preparations. This observation suggests that both the TG traces shown in Figure 6 exhibit comparable modulations from low-frequency, rapidly damped modes. As

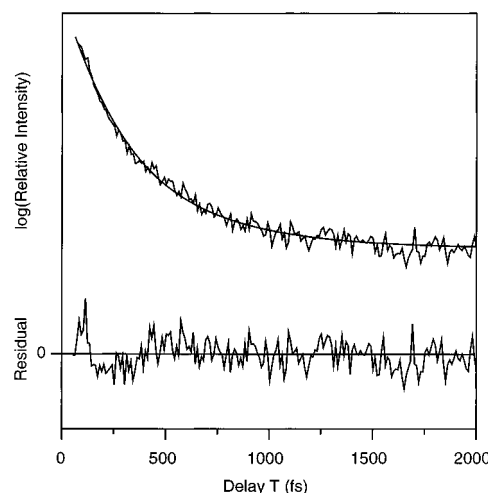


Figure 8. Decaying portion of the TG signal obtained at room temperature with allophycocyanin trimers. The smooth curve drawn through the experimental trace is a fitted curve obtained from a nonlinear least-squares analysis using a multiexponential model; the fit parameters are listed in Table 4. Note that the signal and fit are drawn by using a logarithmic vertical axis. The residual trace shown in the lower portion of the panel is drawn with a linear vertical axis with an arbitrary relative scaling relative to the TG signal shown above it.

TABLE 4: Exponential Fit Components for the TG Signal Obtained at Room Temperature with Allophycocyanin Trimers

	rel amplitude	TG time constant, fs	kinetic time constant, fs ^a	assignment
1	0.52 ± 0.056	160 ± 18	320 ± 36	vibrational relaxation in the lower exciton state
2	0.26 ± 0.028	430 ± 58	860 ± 116	incoherent site-to-site energy transfer
3	0.22 ± 0.012	nondecaying	1.6 ns^b	ground-state recovery

^a The kinetic time constant is twice the corresponding decay time constant observed in the transient-grating signal. ^b From pump-probe and fluorescence decays in other works.^{41,42}

will be discussed below, we suggest that these modulations arise from the inertial solvation response of the protein matrix.

Discussion

The solvent medium dynamics that afford a solute's $|g\rangle \rightarrow |e\rangle$ electronic absorption line its shape, as convolved with the underlying vibrational mode structure, can be described by a Bohr ($|e\rangle - |g\rangle$ transition) frequency time-correlation function $M(t) = \langle \Delta\omega(0)\Delta\omega(t) \rangle / \langle \Delta\omega^2 \rangle$, where $\omega(t)$ represents the transition frequency for the $|g\rangle \leftrightarrow |e\rangle$ transition at a given time t , $\Delta\omega(t) = \omega(t) - \langle \omega_{eg} \rangle$ is the transition frequency averaged over the ensemble.⁴³ In practice, the $M(t)$ function can be composed of a series of terms describing irreversible memory loss due to fluctuations of the $|e\rangle - |g\rangle$ frequency arising from solvent-chromophore collision-like interactions. Recurrences in the $|e\rangle - |g\rangle$ frequency associated with underdamped intramolecular modes are included in $M(t)$ as a series of exponentially damped cosinusoids. Although the diffusional solvation phase is described in $M(t)$ by an exponential term, the broad distribution of solvent modes in the inertial term has been described as a Gaussian component^{2,4,10} or as a very rapidly damped cosinusoid.⁵

Fleming and co-workers² have shown that $M(t)$ can be determined almost directly from the 3PEPS profile, the dependence on the population period T (that spaces the second and

third pulses) of the shift of the integrated stimulated photon-echo signal maximum from time zero, as scanned with respect to the delay t between the first two pulses. In the high-temperature limit and with the assumption of linear response, the 3PEPS profile is proportional to the solvent-response function $S(t) = (\Delta\omega(t) - \Delta\omega(\infty))/(\Delta\omega(0) - \Delta\omega(\infty))$, which describes the dynamic Stokes shift of the stimulated emission or fluorescence.²

The 3PEPS profile, in general, exhibits an initial fast decay on the <10-fs time scale that arises, in the view of Wiersma and co-workers, from pulse-bandwidth-related interference phenomena involving excitation of a near continuum of intrachromophore vibrational modes^{44–46} that are weakly coupled to the electronic transition; accordingly, $M(t)$ is not well described by the initial portion of the 3PEPS profile.^{47,48} An alternative way of describing this, as suggested by the simulations of Fleming and co-workers, is that the initial decay of the 3PEPS profile arises from destructive interference between intramolecular vibrational wave packets.^{3,49} The latter thinking makes it seem natural to associate the first phase of the 3PEPS decay to the time scale of structural displacement when excitation to higher energy of the 0–0 transition energy is employed. In the 3PEPS work described in this paper, we observe a ~16-fs phase of decay that most likely corresponds to this component of the intramolecular vibrational response. This time scale is no doubt lengthened from the true time scale owing to our use of 90-fs pulses in the experiment.

The transient grating (TG) signal mimics the decay of the 3PEPS time profile except that it also depends on population. The TG signal decays as the excited-state portion of the population grating shifts partially off resonance owing to dynamic solvation or radiationless decay. The ground-state recovery is typically on the nanosecond time scale for the systems to be considered here, so the TG signal exhibits a long-lived offset that cannot be distinguished from a long-lived portion of $M(t)$ that arises, say, from static inhomogeneity.³

Inertial Solvation in Proteins. The results presented in this paper allow us, for the first time, to observe directly the dynamics related to protein-matrix solvation dynamics in the two phycobiliproteins that we studied. The idea that protein-matrix solvation dynamics occur on the <100-fs time scale in the α subunit of *C*-phycocyanin was previously inferred from a modeling of time-resolved absorption-difference spectra in terms of photobleaching (PB), stimulated-emission (SE), and excited-state absorption components.¹⁸ The SE component exhibits a dynamic Stokes shift over a ~700 cm^{-1} range, with most of the shift complete within 200 fs; however, the final position of the SE maximum (as observed at a 1-ps delay) is only about 90% shifted from the origin to the equilibrium position, as defined by the maximum of the continuous fluorescence-emission spectrum. This observation led to the suggestion that the solvation response of the protein matrix is biphasic, in analogy to the response of molecular liquids. The slower, diffusional phase of the protein-matrix response was inferred to be very slow because collective or conformational motions are involved.¹⁸ The time scale suggested for the inertial phase, in contrast, was on almost the same time scale as that observed for molecular liquids such as water and acetonitrile using femtosecond fluorescence upconversion.^{11,12}

The new third-order spectroscopic methods used in this paper return dynamical information in a manner that is independent of modeling of the SE line shape. The part of the 3PEPS profile observed in the α -subunit and allophycocyanin trimers that involves the inertial part of the protein-matrix solvation response

is on the 80–100-fs time scale. This component is cleanly resolved from the fastest phase of the 3PEPS profile. A comparable phase of response was observed by Fleming and co-workers with a 50–70-fs time constant in the 3PEPS profile of the dye IR144 in several solvents.^{4,5} The TG traces indicate the presence of a rapidly damped 72- cm^{-1} modulation that accounts for modulation on the same time scale as the 80–100-fs component in the 3PEPS profile. Thus, it may be possible to model the inertial response using a 72- cm^{-1} modulation in lieu of a Gaussian profile with a decaying tail with an apparent 80–100-fs time constant. This suggestion is prompted, in part, by recent work by Fleming and co-workers, in which the inertial solvation part of $M(t)$ for IR144 was modeled with a 60- cm^{-1} solvent mode, with the vibrational dephasing time on the <200-fs time scale.⁵

We should point out here that the inertial phase of the response detected in the 3PEPS profile with α -subunit preparations does not involve the bulk aqueous solvent. In a separate contribution,¹⁹ we describe the use of solvent perturbation spectroscopy to show that the phycocyanobilin chromophore's π electrons are effectively shielded from bulk solvent dipoles. The polarity of the surrounding solvent can be lowered significantly by addition of methanol, for instance, without causing a solvatochromic shift of the continuous absorption or fluorescence spectra of the phycocyanobilin chromophore. At high methanol concentrations, however, the conformation of the protein abruptly changes to a state in which the chromophore is bathed in the external solvent.¹⁹ We conclude for now that the inertial solvation response involves librational motion of polar amino acid side chains and, perhaps, included water molecules. This is a *general* proposal; as an example, we suggest that the ultrafast protein-matrix solvation dynamics around the blue copper site in plastocyanin, as inferred by Loppnow and co-workers^{50,51} from resonance Raman excitation profiles, involve an inertial response.

Diffusive Solvation. The slow phase of the 3PEPS profile observed with α -subunit preparations involves a decay on at least the ~5-ps time scale. It can be assigned, by default, to the diffusional solvation response of the protein matrix. A 20-ps component that probably arises from this portion of the solvation response is observed in the TG signal. 3PEPS experiments with delays T over the 1–100-ps range show that 3 fs of the total shift in α -subunit preparations occurs beyond the 100-ps time scale. A comparable offset in the 3PEPS profile arising from inhomogeneity was observed by Fleming and co-workers in their study of IR144 dissolved in a glass formed from the organic polymer poly(methyl methacrylate) (PMMA); in that work, it is interesting that no diffusional phase of solvation response was observed.⁵

The slowly decaying TG signal and the offset in the 3PEPS profile involve a long-lived inhomogeneity that most likely arises from a distribution of protein conformations that interconvert over a broad range of time scales. Work by Pierce and Boxer⁵² and by McLendon, Mukamel, and co-workers⁵³ on solvation dynamics in heme proteins shows that the dynamic Stokes shift of the fluorescence of an extrinsic probe spans several orders of magnitude of delay out to at least the nanosecond regime. To characterize the diffusional response further, it will be necessary to characterize the 3PEPS profile or TG decay under conditions that affect the conformational state of the protein or that affect the motions of the outside of the protein. We plan to present in a separate contribution a full analysis of the $M(t)$ function determined from 3PEPS profiles measured in viscous

solutions, in binary methanol/water solutions, and as a function of temperature.⁵⁴

Interexciton-State Radiationless Decay and Exciton-State Correlation in Allophycocyanin. The 3PEPS profile exhibited by allophycocyanin trimers at room temperature does not exhibit a long-lived offset. In addition to the components in the 3PEPS profile that can be assigned to dynamics of an isolated phycocyanobilin chromophore in a biliprotein-derived binding site, allophycocyanin exhibits fast components in the 3PEPS profile arising from chromophore–chromophore interactions. The 3PEPS results, in particular, prove that extremely fast radiationless decay channels transfer population between the exciton states that arise from the paired phycocyanobilin chromophores. This transfer of population occurs on a time scale that is at least an order of magnitude faster than that predicted for Förster energy transfer in the weak-coupling limit.

The 622-nm pump pulses used in the 3PEPS experiment prepare a $\sim 3:1$ ratio of the two exciton states (see Figure 3) that contribute to allophycocyanin's absorption spectrum.²⁸ Population is rapidly transferred between the exciton states, mostly in a downward direction, until a Boltzmann population distribution over the two states is established.^{55,56} Previous results, based on transient hole-burning spectroscopy and on femtosecond anisotropy decays, suggest that the effective time constant for this transfer of population is on the 10–60-fs time scale. A red-shifted PB/SE spectrum forms on the 30–60-fs time scale owing to net population of the lower exciton state from the upper exciton state.²⁷ Two-color anisotropy decays, using 620-nm pump and 640-nm probe pulses, exhibit a 10–30-fs decay component from a large initial anisotropy that was assigned to the interference between Feynmann paths involving the two exciton states.²⁶ Given the time-resolved spectral information, this fast anisotropy component was assigned to interexciton-state radiationless decay rather than to the other contribution to the anisotropy decay (using the theory of Wynne and Hochstrasser^{57–59} and of Knox and Gülen⁵⁶) from incoherent energy transfer between chromophore sites. Note that these theories do not predict a priori which phase of the anisotropy response should be faster; Galli et al.⁵⁹ accordingly obtained two possible assignments for the anisotropy decay observed in magnesium tetraphenylporphyrin involving the near-degenerate Q_y states. In the case of allophycocyanin, however, we were able to assign the faster of the two phases of the anisotropy decay to interexciton-state radiationless decay owing to the independent observation of a corresponding spectral relaxation on that time scale.^{26–28}

Consistent with these previously reported observations, the 3PEPS profile for allophycocyanin trimers exhibits a component with a ~ 56 -fs time constant that apparently directly reports the contribution to dephasing from interexciton-state radiationless decay between the $|+\rangle$ and $|-\rangle$ state manifolds. The true time constant and functional form of the contribution of this radiationless decay path to the $M(t)$ function for allophycocyanin has to be determined by numerical modeling,⁴ which we intend to present in a separate contribution along with a study of the dependence on temperature.⁶⁰ The 3PEPS results account for the observation that the *promptly red-shifted* PB/SE spectrum observed in the transient hole-burning spectrum exhibits line broadening owing to transient solvation on ~ 100 -fs time scale.²⁸ The time constant for interexciton-state radiationless decay obtained from the 3PEPS profile is about a factor of 2 shorter than that determined for inertial solvation (80–100-fs).

Up to this point we have treated allophycocyanin as binding a set of *isolated* chromophore dimers that are related by the C_3

symmetry axis. This is a reasonable first approximation, given the large radial separation between the pairs.²⁴ Owing to the nonnegligible transition dipole–dipole interaction between the pairs, however, the $|+\rangle$ or $|-\rangle$ pair exciton states are actually split further into a manifold of three states. It is attractive to assign the ~ 220 -fs 3PEPS component to interexciton-state radiationless decay between states in either the $|+\rangle$ or $|-\rangle$ manifolds. This time scale is much too short to arise from *incoherent* (Förster-type) energy transfer between the pairs or even between the chromophores in a given pair. The former time scale has been directly measured by Beck and Sauer to occur on the 210-ps time scale;⁴¹ calculations by Sauer and Scheer suggest that the latter process occurs on the 700-fs time scale in the related, *C*-phycocyanin system (*vide infra*).⁶¹

We may be able to test the assignment of the ~ 220 -fs 3PEPS component by performing a comparable study of allophycocyanin B, another component of the core of the phycobilisome. The trimeric form of allophycocyanin B represents a severe distortion from C_3 symmetry; one of the three pairs of phycocyanobilin chromophores is red-shifted, owing to the presence of an α subunit that is different from the other two in the trimer.^{62–64} This distortion will cause a larger splitting in the $|+\rangle$ or $|-\rangle$ manifolds, perhaps large enough to be detected in time-resolved pump–probe spectra.

The presence of components in the allophycocyanin's 3PEPS profile from interexciton-state radiationless decay is interesting in that these components arise physically from protein-matrix fluctuations. In the limit of infinitely strong coupling, the upper and lower exciton states of a pair of chromophores are *correlated*, so a radiationless transfer of population between the two states would not contribute to decay of $M(t)$. This is to be compared to the limit of weak coupling, where radiationless decay between the two states actually involves incoherent energy transfer between the two site (isolated chromophore) states; owing to a lack of correlation of the site energies with respect to fluctuations arising from solvent perturbations, $M(t)$ may exhibit a decay on the time scale of incoherent energy transfer.^{1,65} The fact that a decay occurs on the time scale inferred from previous measurements for interexciton-state radiationless decay shows that the upper and lower exciton-state manifolds are *not* perfectly correlated. This conclusion is consistent with the relative magnitude of the transition-dipole–dipole interaction strength between the $\alpha 84$ and $\beta 84$ chromophores in a given pair (~ 150 cm⁻¹²⁸) and the observed widths of the exciton-state transitions (~ 470 cm⁻¹ for the $|+\rangle$ band and ~ 1700 cm⁻¹ for the $|-\rangle$ band²⁷), which implies that this system is at best in the intermediate coupling limit. Of course, the two exciton-state manifolds are well enough correlated to be *ordered* so that holes are burned to the red of the pump wavelength when the pump wavelengths over the 620–645-nm range are employed. In addition, the initial and final position of the holes track the pump wavelength as it is tuned over the 620–645-nm region of the spectrum. These results can only be explained by a exciton-coupling picture.²⁸

A comparable degree of imperfect correlation between exciton states has been detected by Small and co-workers in the primary electron donor of the purple-bacterial reaction center⁶⁶ and in the bacteriochlorophyll *a* antenna complex of *Prosthecochloris aestuarii*.⁶⁷ In these systems, however, state correlation was judged from the degree of tracking of satellite hole features in persistent nonphotochemical hole-burning spectroscopy at low temperature. The present work on allophycocyanin suggests that the 3PEPS method affords an alternative approach for the

study of state correlation that can be exploited even at physiological temperatures.

Vibrational Relaxation and Incoherent Energy Transfer in Allophycocyanin. The TG signal observed with allophycocyanin trimers reports dynamics on a longer time scale than can be retrieved from the 3PEPS profile. Although the ~ 28 and 110-fs components to be anticipated in the TG decay from interexciton-state radiationless decay of the two types discussed above are too short to be clearly resolved from the instrument-response function owing to the use of 90-fs pulses, the TG decay directly reports two processes that occur on a longer time scale. The fraction of population placed in the lower exciton state by the 620-nm pump pulses used in the present 3PEPS and TG experiments is initially deposited in the $\nu = 1$ level of the $\sim 1500\text{-cm}^{-1}$ pyrrole-stretching vibration.²⁸ Vibrational relaxation contributes to the decay of the excited-state portion of the grating for this fraction of population. The previously reported transient hole-burning results show that a $\sim 300\text{--}400$ -fs decay arises from vibrational relaxation from the $\nu = 1$ level.^{27,28} The TG decay exhibits a ~ 160 -fs component that reports the presence of a ~ 320 -fs population decay.

As discussed above, we currently favor assignment of the ~ 220 -fs 3PEPS component detected in allophycocyanin trimers to interexciton-state relaxation dynamics in either the $|+\rangle$ or $|-\rangle$ manifolds rather than to vibrational relaxation from the $\nu = 1$ level. While the 220-fs time scale observed in the 3PEPS profile is on a comparable time scale, the $\nu = 0$ and $\nu = 1$ levels in a given electronic state's manifold ought to be well correlated with respect to solvent fluctuations. Accordingly, it is not obvious that population transfer between the vibrational levels will contribute to the 3PEPS transient. This issue has not yet been explored in any 3PEPS study, to our knowledge. The TG transient exhibits a ~ 430 -fs exponential component that reports a ~ 860 -fs kinetic component that can be assigned to incoherent energy transfer between the chromophores in a given pair. The slow part of the anisotropy decay observed with allophycocyanin trimers exhibits components with time constants distributed over the 400-fs to 1-ps time scale²⁶ that can now be reasonably assigned to intrapair energy transfer.

Last, we have previously discussed the possibility that localization, a radiationless transition from the exciton (delocalized) states to one of the site (localized) states corresponding to one of the chromophores in a pair, should make a contribution to the dynamics in allophycocyanin trimers.^{27,28} We previously attributed to localization a ~ 1.2 -ps component observed in a two-color pump-probe experiment that was conducted so as to be insensitive to vibrational relaxation (with 655-nm pump pulses that directly prepare the lower exciton state near, or below, the 0-0 transition's energy).²⁸ Unfortunately, in the present work, owing to the use of 622-nm excitation, we did not observe any components on the ~ 1.2 -ps time scale in the TG signal, and the 3PEPS profile decays to the noise level owing to population relaxation much too rapidly to permit even observation of the ~ 860 -fs component that is assigned above to intrapair energy transfer. The nonexponential character of the 100-1000-fs part of the TG decay observed with allophycocyanin trimers, however, suggests the presence of many different time scales of response, so it is probably unreasonable to try to account for the decay in terms of just the two discrete components fitted to the transient shown in Figure 8.

Conclusions

Our results show that the third-order spectroscopies used in this work return complementary but superior information on

the components of $M(t)$ for the phycocyanobilin chromophores in the α -subunit and allophycocyanin systems. As suggested by the work by Fleming and co-workers,^{2,3} the 3PEPS profiles directly return information on the fastest dynamics. We observe components in the 3PEPS profiles that allow distinction between the part of the dynamic Stokes shift arising from vibrational displacement from that involved in inertial solvation. This work establishes clearly, for the first time, that an inertial solvation component that is analogous to that present in molecular solvents arises from the protein-matrix surroundings of an imbedded chromophore. In addition, in allophycocyanin trimers, the exquisitely fast dynamics arising from interexciton-state radiationless decay are detected here for the first time in a manner that is independent of conjecture of the shape of the two overlapped exciton-state absorption bands. In contrast, the TG signals observed with both systems are apparently more sensitive to the slower dynamical components that the 3PEPS profiles have difficulty reporting owing to signal/noise limitations. It is also interesting that the TG signals directly reveal dynamics that are related to the inertial protein-matrix solvation response in terms of rapidly damped modulations. Further, the TG signals appear to be more sensitive than is the 3PEPS profile to the solvation dynamics that arise from conformational diffusion.

Acknowledgment. This work was supported by the United States Department of Agriculture (NRICGP). B.J.H. and W.M.D. were supported by National Institutes of Health graduate traineeships in Molecular Biophysics. M.D.E. was supported by a graduate fellowship from the David and Lucile Packard Foundation. We are grateful to Professor Anne Myers (University of Rochester) for providing us access to the LPSVD analysis program.

References and Notes

- (1) Joo, T.; Jia, Y.; Yu, J.-Y.; Jonas, D. M.; Fleming, G. R. *J. Phys. Chem.* **1996**, *100*, 2399-2409.
- (2) Cho, M.; Yu, J.-Y.; Joo, T.; Nagasawa, Y.; Passino, S. A.; Fleming, G. R. *J. Phys. Chem.* **1996**, *100*, 11944-11953.
- (3) Joo, T.; Jia, Y.; Yu, J.-Y.; Lang, M. J.; Fleming, G. R. *J. Chem. Phys.* **1996**, *104*, 6089-6108.
- (4) Passino, S. A.; Nagasawa, Y.; Joo, T.; Fleming, G. R. *J. Phys. Chem. A* **1997**, *101*, 725-731.
- (5) Nagasawa, Y.; Passino, S. A.; Joo, T.; Fleming, G. R. *J. Chem. Phys.* **1997**, *106*, 4840-4852.
- (6) Weiner, A. M.; Ippen, E. P. *Chem. Phys. Lett.* **1985**, *114*, 456-460.
- (7) Fourkas, J. T.; Fayer, M. D. *Acc. Chem. Res.* **1992**, *25*, 227-233.
- (8) de Boeij, W. P.; Pshenichnikov, M. S.; Wiersma, D. A. *Chem. Phys. Lett.* **1995**, *238*, 1.
- (9) Pshenichnikov, M. S.; Duppen, K.; Wiersma, D. A. *Phys. Rev. Lett.* **1995**, *74*, 674-677.
- (10) de Boeij, W. P.; Pshenichnikov, M. S.; Wiersma, D. A. *J. Phys. Chem.* **1996**, *100*, 11806-11823.
- (11) Rosenthal, S. J.; Xie, X.; Du, M.; Fleming, G. R. *J. Chem. Phys.* **1991**, *95*, 4715-4718.
- (12) Jimenez, R.; Fleming, G. R.; Kumar, P. V.; Maroncelli, M. *Nature* **1994**, *369*, 471-473.
- (13) Maroncelli, M.; Kumar, P. V.; Papazyan, A.; Horng, M. L.; Rosenthal, S. J.; Fleming, G. R. In *Ultrafast Reaction Dynamics and Solvent Effects*; Guaduel, Y., Rossky, P. J., Eds.; AIP Press: Woodbury, NY, 1994; pp 310-333.
- (14) Stratt, R. M.; Cho, M. *J. Chem. Phys.* **1994**, *100*, 6700-6708.
- (15) Ladanyi, B. M.; Stratt, R. M. *J. Phys. Chem.* **1995**, *99*, 2502-2511.
- (16) Stratt, R. M.; Maroncelli, M. *J. Phys. Chem.* **1996**, *100*, 12981-12996.
- (17) Riter, R. E.; Edington, M. D.; Beck, W. F. In *Ultrafast Phenomena X*; Barbara, P., Knox, W., Zinth, W., Fujimoto, J., Eds.; Springer-Verlag: Berlin, 1996; pp 324-325.
- (18) Riter, R. E.; Edington, M. D.; Beck, W. F. *J. Phys. Chem.* **1996**, *100*, 14198-14205.
- (19) Homoele, B. J.; Beck, W. F. *Biochemistry* **1997**, *36*, 12970-12975.

- (20) Glazer, A. N. *Annu. Rev. Biophys. Biophys. Chem.* **1985**, *14*, 47–77.
- (21) Schirmer, T.; Bode, W.; Huber, R.; Sidler, W.; Zuber, H. *J. Mol. Biol.* **1985**, *184*, 257–277.
- (22) Schirmer, T.; Huber, R.; Schneider, M.; Bode, W.; Miller, M.; Hackert, M. L. *J. Mol. Biol.* **1986**, *188*, 651–676.
- (23) Schirmer, T.; Bode, W.; Huber, R. *J. Mol. Biol.* **1987**, *196*, 677–695.
- (24) Brejc, K.; Ficner, R.; Huber, R.; Steinbacher, S. *J. Mol. Biol.* **1995**, *249*, 424–440.
- (25) Kraulis, P. J. *J. Appl. Crystallogr.* **1991**, *24*, 946–950.
- (26) Edington, M. D.; Riter, R. E.; Beck, W. F. *J. Phys. Chem.* **1995**, *99*, 15699–15704.
- (27) Edington, M. D.; Riter, R. E.; Beck, W. F. *J. Phys. Chem.* **1996**, *100*, 14206–14217.
- (28) Edington, M. D.; Riter, R. E.; Beck, W. F. *J. Phys. Chem. B* **1997**, *101*, 4473–4477.
- (29) Riter, R. E.; Edington, M. D.; Beck, W. F. *J. Phys. Chem. B* **1997**, *101*, 2366–2371.
- (30) van der Zwan, G.; Hynes, J. T. *J. Phys. Chem.* **1985**, *89*, 4181–4188.
- (31) Simon, J. D. *Acc. Chem. Res.* **1988**, *21*, 128–134.
- (32) Alavi, D. S.; Hartman, R. S.; Waldeck, D. H. *J. Chem. Phys.* **1991**, *94*, 4509–4520.
- (33) Glazer, A. N.; Fang, S. *J. Biol. Chem.* **1973**, *248*, 659–662.
- (34) Glazer, A. N.; Fang, S. *J. Biol. Chem.* **1973**, *248*, 663–671.
- (35) Glazer, A. N.; Fang, S.; Brown, D. M. *J. Biol. Chem.* **1973**, *248*, 5679–5685.
- (36) Scherer, N. F.; Ziegler, L. D.; Fleming, G. R. *J. Chem. Phys.* **1992**, *96*, 5544–5547.
- (37) Johnson, A. E.; Myers, A. B. *J. Chem. Phys.* **1996**, *104*, 2497–2507.
- (38) Szalontai, B.; Gombos, Z.; Csizmadia, V.; Csatorday, K.; Lutz, M. *Biochemistry* **1989**, *28*, 6467–6472.
- (39) Szalontai, B.; Gombos, Z.; Csizmadia, V.; Bagyinka, C.; Lutz, M. *Biochemistry* **1994**, *33*, 11823–11832.
- (40) Szalontai, B.; Gombos, Z.; Lutz, M. *Photochem. Photobiol.* **1994**, *59*, 574–578.
- (41) Beck, W. F.; Sauer, K. *J. Phys. Chem.* **1992**, *96*, 4658–4666.
- (42) Debreczeny, M. P.; Sauer, K.; Zhou, J.; Bryant, D. A. *J. Phys. Chem.* **1993**, *97*, 9852–9862.
- (43) Mukamel, S. *Principles of Nonlinear Optical Spectroscopy*; Oxford University Press: New York, 1995.
- (44) Lorincz, A.; Novak, F. A.; Rice, S. A. In *Ultrafast Phenomena IV*; Auston, D. H., Eistenthal, K. B., Eds.; Springer-Verlag: Berlin, 1984; pp 387–389.
- (45) Becker, P. C.; Fragnito, H. L.; Bigot, J.-Y.; Brito Cruz, C. H.; Fork, R. L.; Shank, C. V. *Phys. Rev. Lett.* **1989**, *63*, 505–507.
- (46) Bigot, J.-Y.; Portella, M. T.; Schoenlein, R. W.; Bardeen, C. J.; Migus, A.; Shank, C. V. *Phys. Rev. Lett.* **1991**, *66*, 1138–1141.
- (47) de Boeij, W. P.; Pshenichnikov, M. S.; Wiersma, D. A. *Chem. Phys. Lett.* **1996**, *253*, 53–60.
- (48) de Boeij, W. P. Ph.D. Thesis, University of Groningen, 1997.
- (49) Fleming, G. R.; Cho, M. *Annu. Rev. Phys. Chem.* **1996**, *47*, 109–134.
- (50) Fraga, E.; Webb, M. A.; Loppnow, G. R. *J. Phys. Chem.* **1996**, *100*, 3278–3287.
- (51) Loppnow, G. R.; Fraga, E. *J. Am. Chem. Soc.* **1997**, *119*, 896–905.
- (52) Pierce, D. W.; Boxer, S. G. *J. Phys. Chem.* **1992**, *96*, 5560–5566.
- (53) Bashkin, J. S.; McLendon, G.; Mukamel, S.; Marohn, J. *J. Phys. Chem.* **1990**, *94*, 4757–4761.
- (54) Hmoelle, B. J.; Beck, W. F., manuscript in preparation.
- (55) Rahman, T. S.; Knox, R. S.; Kenkre, V. M. *Chem. Phys.* **1979**, *44*, 197–211.
- (56) Knox, R. S.; Gülen, D. *Photochem. Photobiol.* **1993**, *57*, 40–43.
- (57) Wynne, K.; Hochstrasser, R. M. *Chem. Phys.* **1993**, *171*, 179–188.
- (58) Wynne, K.; Hochstrasser, R. M. *J. Raman Spectrosc.* **1995**, *26*, 561–569.
- (59) Galli, C.; Wynne, K.; LeCours, S.; Therien, M. J.; Hochstrasser, R. M. *Chem. Phys. Lett.* **1993**, *206*, 493–499.
- (60) Hmoelle, B. J.; Beck, W. F., manuscript in preparation.
- (61) Sauer, K.; Scheer, H. In *Photosynthetic Light-Harvesting Systems*; Scheer, H., Schneider, S., Eds.; Walter de Gruyter: Berlin, 1988; pp 507–511.
- (62) Maxson, P.; Sauer, K.; Zhou, J.; Bryant, D. A.; Glazer, A. N. *Biochim. Biophys. Acta* **1989**, *977*, 40–51.
- (63) Maxson, P. Ph.D. Thesis, University of California, Berkeley, 1988.
- (64) Glazer, A. N. In *Cyanobacteria*; Packer, L., Glazer, A. N., Eds.; Academic Press: San Diego, 1988; Vol. 167; pp 291–303.
- (65) Jimenez, R.; van Mourik, F.; Yu, J. Y.; Fleming, G. R. *J. Phys. Chem. B* **1997**, *101*, 7350–7359.
- (66) Johnson, S. G.; Tang, D.; Jankowiak, R.; Hayes, J. M.; Small, G. H. *J. Phys. Chem.* **1989**, *93*, 5953–5957.
- (67) Johnson, S. G.; Small, G. H. *J. Phys. Chem.* **1991**, *95*, 471–479.